



Contents lists available at ScienceDirect

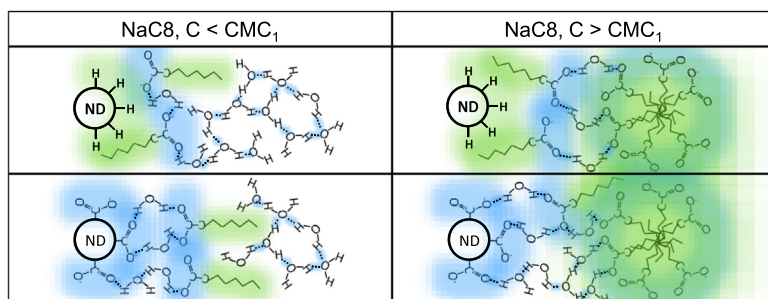
Journal of Colloid and Interface Science

journal homepage: www.elsevier.com/locate/jcis

Nanodiamonds and surfactants in water: Hydrophilic and hydrophobic interactions

Alexey M. Vervalde^{a,*}, Kirill A. Laptinskiy^b, Sergey A. Burikov^a, Tatiana V. Laptinskaya^a, Olga A. Shenderova^c, Igor I. Vlasov^{d,e}, Tatiana A. Dolenko^{a,e}^aPhysical Department, M.V. Lomonosov Moscow State University, 1 bldg. 2 Leninskie Gory, 119991 Moscow, Russia^bSkobeltsyn Institute of Nuclear Physics, M.V. Lomonosov Moscow State University, 1 bldg. 2 Leninskie Gory, 119991 Moscow, Russia^cAdamas Nanotechnologies, Inc., Raleigh, 8100 Brownleigh Dr, Raleigh, NC 27617, USA^dA.M. Prokhorov General Physics Institute of Russian Academy of Sciences, 38 Vavilov st., 119991 Moscow, Russia^eNational Research Nuclear University MEPhI, 31 Kashirskoe shosse, 115409 Moscow, Russia

GRAPHICAL ABSTRACT



ARTICLE INFO

Article history:

Received 1 February 2019

Revised 28 March 2019

Accepted 30 March 2019

Available online 30 March 2019

Keywords:

Hydrophobic nanodiamonds

Hydrophilic nanodiamonds

Surfactants

Hydrogen bonds

Micellization

Raman spectra

ABSTRACT

Hypothesis: Nanodiamonds, one of the most promising nanomaterials for the use in biomedicine, placed in the organisms are bound to interact with various amphiphilic lipids and their micelles. However, while the influence of surfactants, the close relative of lipids, on the properties of colloidal nanodiamonds is well studied, the influence of nanodiamonds on the properties of surfactants, lipids, and, therefore, on the structure of surrounding tissues, is poorly understood.

Experiment: In this work, the influence of interactions of hydrophobic and hydrophilic nanodiamonds with ionic surfactant sodium octanoate in water on hydrogen bonds, the properties of the surfactant and micelle formation were studied using Raman spectroscopy and dynamic light scattering technique.

Findings: Nanodiamonds are found to actively influence the bulk properties only of the pre-micellar surfactant solutions: the strength of hydrogen bonds, ordering and conformation of hydrocarbon tails, the critical micelle concentration. This influence is deduced to be dependent on two mechanisms not unique to nanodiamonds: (1) the induction of micro-flows around nanoparticles undergoing Brownian motions, and (2) the creation of the chaotic state in the surfactant solutions if two or more incompatible types of interactions between nanoparticles' surfaces and surfactants are similarly favorable, e.g. hydrophobic interaction and Coulomb attraction.

© 2019 Elsevier Inc. All rights reserved.

Abbreviations: ND, nanodiamond; NaC8, sodium octanoate; CMC, critical micelle concentration; DLS, dynamic light scattering.

* Corresponding author.

E-mail address: alexey.vervald@physics.msu.ru (A.M. Vervalde).<https://doi.org/10.1016/j.jcis.2019.03.102>

0021-9797/© 2019 Elsevier Inc. All rights reserved.

1. Introduction

At present, the use of nanomaterials in biology and medicine is actively developing. Carbon nanoparticles, semiconductor quantum dots, complexes with rare earth elements and other nanoparticles are used as luminescent imaging probes, for targeted drug delivery, in regenerative medicine, and as nanosensors of intracellular processes. Nanodiamonds (NDs) occupy a special place among these nanoparticles due to their unique combination of properties – low cost, stable luminescence, chemically active surface, and biocompatibility [1,2].

One of the most important properties of nanodiamonds is their diverse chemically active surface, which provides a wide range of possibilities for their use as drug carriers [3–5], adsorbents [6,7], and bases for the creation of various bioconjugates [8–10]. Through this surface, NDs used in biomedicine as medical agents will inevitably interact with amphiphilic compounds whose micelles are the main structural elements of biological tissues: cell membranes are composed of lipid bilayers, bile acid micelles perform various vital functions, phospholipid renewal is associated with processes of structural micelle membrane recovery, etc. [11]. The biological micelles, however, have the sizes of hundreds of nanometers against the single-digit nanometer nanoparticles. At these ratios and sizes, no microscope or other techniques can provide viable information on the nanoscale influence of nanoparticles on the properties of micelles.

The insight in the nanoscale features of interactions between nanoparticles and biological micelles can be obtained by studying the interactions of nanoparticles with close relatives of amphiphilic lipids – surfactants, which at certain concentrations form micelles [12–14]. Unfortunately, large number of the studies on the systems of nanoparticles with surfactants concerns the properties of nanoparticles, the efficiency of the usage of surfactants, or in several occasions the influence of nanoparticles on the critical micelle concentration of surfactants [15] and the effect of nanoparticles on the changes of surface tension induced by surfactants [16]. Like that, the nanoparticles charged similarly to the head group of surfactants are determined to repulse surfactant from the bulk of the suspensions to the water/air interface [16], but in literature there is no information on the influence of nanoparticles on the nanoscale structure of the surfactant themselves.

The majority of publications devoted to the study of the interaction of nanodiamonds and surfactants in suspensions concerns the effect of surfactant on the dispersibility of the NDs [17–21]. Surfactants are actively adsorbed on the surface of NDs, changing their zeta potential and aggregation properties [22–25]. Two mechanisms of surfactant adsorption on NDs, according to which the same surfactant can interact in different ways with different parts of the ND surface, were proposed [17,18]. The first mechanism is the hydrophobic interaction between hydrophobic surfactant tails and hydrophobic regions of the ND surface, leading to partial hydrophilization of the surface. The second is Coulomb attraction in the case of an ionic surfactant and an oppositely charged surface of NDs, which leads to partial hydrophobization of the surface. It was noted that other molecules of the surfactant can interact with such a hydrophobic surface, forming an analog of a double layer around NDs [18]. In any event, the addition of surfactants provides an improvement in the dispersibility of NDs not only in aqueous solutions but also in cells, which expands the prospects of their biological application [18,23].

According to the results of many authors [26–33], nanodiamonds significantly change the structure of the surrounding solvent. As was established by X-ray pair distribution function analysis, colloidal nanoparticles induce restructuring and (dis) ordering of the molecules of the polar and non-polar solvents

surrounding them at a distance of up to 2 nm [26]. More specific for NDs, in 2007, by the differential scanning calorimetry of melting the aqueous gel of nanodiamonds, the special nanosized phase of water around nanodiamonds was found [27]. Batsanov et al. confirmed the existence of that stable water shell, showed that its thickness is about 0.5 nm around nanodiamonds in water and that the shell properties differ significantly from the properties of bulk water so that even “traces of ND drastically affect the physical properties of water” [28,29]. It was concluded that NDs cause a structural rearrangement of water molecules at large distances, not only in nearest shells, most likely through an orientation polarization mechanism. The effect of dispersed nanodiamonds on the properties of a bulk solvent has been shown: dispersed nanodiamonds weaken hydrogen bonds in bulk water, and the change in energy of the hydrogen bonds depends on the type of diamond surface groups [30–32]. In contrast to suspensions of hydrophilic carboxylated NDs, in suspensions of hydrophobic hydrogenated nanodiamonds a long-range disruption of the water hydrogen bonds is observed, even when such NDs do not form hydrogen bonds directly with surrounding solvent molecules. However, in our previous study [34] we have demonstrated that surfactants can “shield” the hydrogen bonds in the suspension from the weakening influence of NDs.

Despite the fact that the surfactants have been used to increase the dispersibility of nanodiamonds for a long time the interactions of nanoparticles with surfactant molecules and the influence of these interactions on the properties of NDs, surfactant, and their environment is far from full understanding. Meanwhile, an understanding of the processes that occur when the NDs are dispersed in water in the presence of surfactants and when such nanoparticles are internalized into the biological material is extremely important for the creation of safe medical agents based on nanoparticles.

The most suitable technique for the elucidating the nanoscale changes in the surrounding of NDs is the vibrational spectroscopy due to the fact that Raman spectra of the molecules are dependent on the characteristics of the electronic configuration in the sample which, in turn, is influenced by the molecular conformation and environment. However, Raman spectroscopy is very demanding to the concentration of the oscillating groups. Therefore, in our experiments, the anionic surfactant sodium octanoate was used due to its record-high critical micelle concentration. The choice of this surfactant allowed us to study in detail the influence of nanodiamonds on both pre-micellar and micellar suspensions of surfactant. Summarizing, in this paper, the interactions of detonation nanodiamonds with an ionic surfactant sodium octanoate in water and the effect of these interactions on the properties of the surfactant and solvent, as well as on the process of micelle formation of surfactants in water were investigated. To study the different types of interactions, NDs with surface hydrophilic (–COOH) and hydrophobic (–H) groups were used. The studies were carried out using dynamic light scattering (DLS) and Raman spectroscopy methods.

2. Materials and methods

2.1. Materials

The initial nanodiamond samples purified from the synthesis soot were obtained from the Adámas Nanotechnologies (USA), the used procedures are described in [35]. Functionalization with carboxyl groups and preparation of the initial aqueous suspension of detonation nanodiamonds with a concentration of ND-COOH of 28 g/L were performed in the International Technology Center (USA) by the methods described in [35,36]. Hydrogenation of NDs and the preparation of the initial aqueous suspension of ND-

H with a concentration of 5.3 g/L were carried out in CEA, LIST, Diamond Sensors Laboratory (France) [32].

Sodium octanoate ($C_7H_{15}COO^- Na^+$, NaC8) of a ph. Eur pure class was purchased from AppliChem GmbH (Germany).

2.2. Sample preparation

Bidistilled deionized water with an electrical conductivity of 0.5 $\mu\text{Sm/cm}$ (Milli-Q) was used for the preparation of suspensions. Aqueous suspensions of NDs were prepared with concentrations of 0.5 g/L for ND-COOH and 0.25 g/L for ND-H by diluting the initial NDs suspensions with deionized water. The suspensions were treated in an ultrasound bath (Bandelin Sonorex rk 31) for 30 min. During the experiment, sodium octanoate was gradually added to water and to prepared suspensions of ND-COOH and ND-H so that the concentration of NaC8 (C_{NaC8}) in three samples changes in the range from 0 up to 1700 mM with the steps of 20–100 mM.

2.3. Experimental procedures

To verify ND functional coverage, IR absorption spectra of the samples were obtained using IR spectrometer Varian 640-IR FT-IR with ATR module with diamond crystal. The spectral resolution was 4 cm^{-1} . The IR absorption spectra of ND-H and ND-COOH are presented in Supplementary Materials (Fig. S1).

The sizes of NDs and sodium octanoate (NaC8) micelles in aqueous suspensions were measured by the method of dynamic light scattering (DLS) using device ALV-CGS 5000/6010 (Germany).

Zeta potential of ND suspensions in the presence of surfactant was measured using Malvern ZetaSizer NanoZS (Malvern, Worcestershire, UK).

Raman spectra of the investigated suspensions were obtained by excitation of a sample with an argon laser with a wavelength of 488 nm (400 mW power) in a 90-degree geometry. The system for recording the Raman spectra consisted of a monochromator (Acton 2500i, focal length 500 mm, grating 900 g/mm) and a CCD-camera (Horiba Jobin Yvon, Sincerity-1024x256-OE). The width of the entrance slit was 25 μm , which provided a practical resolution of 1.5 cm^{-1} . To suppress the scattering at an unshifted frequency, an interference filter Semrock was used, which made it possible to approach the excitation line at 488 nm by 100 cm^{-1} . Raman spectra were recorded in the range 400–4500 cm^{-1} . The spectra were normalized to the power of laser radiation, the spectrum accumulation time, detector sensitivity, and to the integral intensity of the OH stretching band.

All experiments were conducted at a temperature of 25 $^\circ\text{C}$, in three repeats. The obtained results are presented with the errors, which represent the instrumental errors or the standard deviation between experiment repeats, whichever is greater.

3. Results and discussion

The interactions of detonation nanodiamonds ND-COOH and ND-H with an ionic surfactant sodium octanoate (NaC8) was studied in water. The changes of Zeta potential of nanodiamonds with the gradual addition of NaC8 and subsequent disaggregation of NDs was studied with the use of ZetaSizer and DLS technique. The influence of NDs and NaC8 on the hydrogen bonds in water as well as the influence of their interactions on the surfactant molecules were investigated using Raman spectroscopy. All studies were carried out at a temperature of 25 $^\circ\text{C}$.

At a specific concentration known as the critical micelle concentration (CMC_1) situated in the range of 300–360 mM [37], the sodium octanoate molecules in water form spherical micelles. In the concentration range of 200–300 mM, preceding CMC_1 , a part

of monomolecules of NaC8 in aqueous solutions is observed to form the dimers with surfactant heads looking in opposite directions. When the CMC_1 is reached, more than a half of the sodium octanoate molecules in solution form spherical micelles. With a further increase in the concentration of NaC8, the number of molecules in the micelles increases. When NaC8 concentration has reached the region of 1.1–1.2 M (known as the second critical micelle concentration (CMC_2)), hydration of hydrocarbon tails inside micelles decreases: the micelles remain spherical, but their packing became denser [37,38]. The depicted ranges of the CMCs on all Figures of this manuscript represent the CMCs ranges according to the literature data for the aqueous solutions of NaC8, without dispersed NDs.

3.1. Disaggregation of NDs in aqueous suspensions in the presence of NaC8

The hydrodynamic radii of the ND-COOH and ND-H aggregates in water and in aqueous solutions of NaC8 with concentrations of $C_{\text{NaC8}} = 200 \text{ mM}$ ($C_{\text{NaC8}} < \text{CMC}_1$) and $C_{\text{NaC8}} = 500 \text{ mM}$ ($C_{\text{NaC8}} > \text{CMC}_1$) were measured using DLS. The size of ND-COOH in water was found to be $12 \pm 1 \text{ nm}$ and did not change in the presence of a surfactant with a concentration of 200 mM. The hydrodynamic radius of ND-H in water was found to be $180 \pm 20 \text{ nm}$. In the presence of 200 mM sodium octanoate, large aggregates of hydrophobic nanodiamonds brake down into small particles with an average size of $24 \pm 2 \text{ nm}$. It should be mentioned that at the pre-micellar concentrations single molecules of NaC8 does not contribute to the scattering and thus are not present in the DLS's size distribution.

When the concentration of NaC8 was increased to $C_{\text{NaC8}} = 500 \text{ mM}$ ($C_{\text{NaC8}} > \text{CMC}_1$), only the signal due to the scattering of simple spherical micelles with a size of $1.0 \pm 0.2 \text{ nm}$ was observed in DLS. At such a surfactant concentration, most of NaC8 molecules either enter the micelles or “surround” the ND particles. The absence of a DLS signal from larger particles can be explained by the fact that the amount of nanodiamonds is extremely small compared to the amount of NaC8 molecules – 10^8 times less. As a result, the signal from nanometer-sized micelles is intense and obscures weak signals from a small number of larger particles.

Measurement of zeta potentials of the studied aqueous suspensions of NDs showed that the presence of surfactants in the suspension of nanoparticles significantly changes their zeta potential (Fig. 1). When NaC8 is added to the suspension, the zeta potential changes from -42.0 mV for ND-COOH and from $+29.2 \text{ mV}$ for ND-

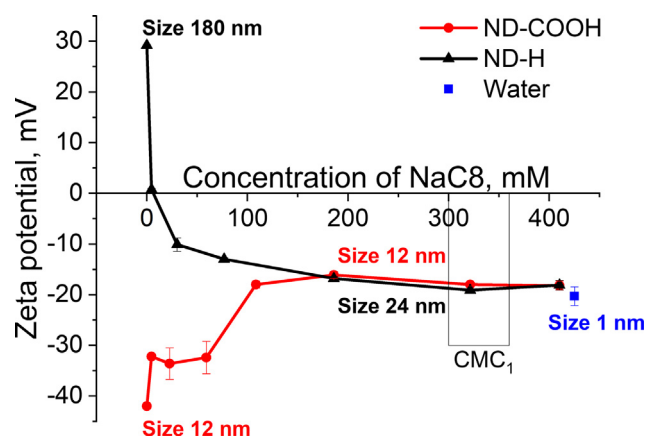


Fig. 1. Dependence of the zeta potentials of ND-H and ND-COOH in aqueous suspensions from the NaC8 concentration combined with the results of DLS measurements. Error bars represent the standard deviation between three repeats of the experiments and in some points are overcast by plotted dots.

H in suspensions without NaC8 to the values similar to NaC8 micelles of -20.3 mV in suspensions with 100-mM NaC8 for both types of nanoparticles. It means that by the interactions with NaC8, nanodiamonds obtain Zeta potential of NaC8 micelles well before the formation of the micelles in the suspensions. According to our spectroscopic results presented below, this effect cannot be attributed to the shift in CMC value of NaC8 (the shift occurs, but not to a such degrees), and instead it indicates the “adsorption” of NaC8 on NDs or, in more accurate terms, the formation of ND-NaC8 systems, the properties of which, instead of the pure NDs, were actually measured. With the addition of NaC8, the dispersibility of ND-H nanoparticles in suspensions increases: their aggregates decompose.

3.2. Raman spectroscopy of aqueous suspensions of NDs and surfactants

Raman spectroscopy is a powerful technique that makes it possible to obtain information about the processes of micelle formation and the structure of supramolecular assemblies in surfactant solutions. As it was established in many works, stretching vibration bands of CH groups are sensitive to the local environment of hydrocarbon tails [39,40]. The relative intensity of bands of symmetric CH vibrations in CH_2 - and CH_3 - groups make it possible to judge the ordering of hydrocarbon tails, and the intensity of asymmetric oscillations of CH in CH_3 - groups can be used to estimate the degree of polarity of the environment of surfactant molecules [39,41]. The spectral range of the C–C bond vibrations makes it

possible to obtain information on the isomerism of hydrocarbon tails [40,42], and the range of stretching vibrations of OH- groups – on the strength and dynamics of hydrogen bonds of a solvent significantly altered by surfactants [14,43].

The molecular interactions of NDs with surfactants in water was studied by Raman spectroscopy. Raman spectra of NaC8 at different concentrations were measured in water, in aqueous suspension of hydrophilic nanodiamonds ND-COOH with a concentration of 0.5 g/L, and in aqueous suspension of hydrophobic nanodiamonds ND-H with a concentration of 0.25 g/L. The concentration of NaC8 varied in the range from 0 to 1700 mM in steps of 20–100 mM.

Fig. 2a shows some of the spectra obtained. The most intense band ν_{OH} , with a maximum at around 3400 cm^{-1} , is the stretching band of water Raman scattering (OH-group vibrations). The bands ν_{CH_x} in the region of $2800\text{--}3100\text{ cm}^{-1}$ correspond to the stretching vibrations of CH of methyl group CH_3 and six methylene groups of CH_2 of sodium octanoate. Then there are bands δ_{CH_x} and δ_{OH} of deformation vibrations of CH- and OH-groups in the region of $1400\text{--}1700\text{ cm}^{-1}$. The lines ν_{CC} related to the C–C bond vibrations of hydrocarbon tails in the “gauche-” and “trans-” conformations are observed in the region of $1000\text{--}1150\text{ cm}^{-1}$. The lines and bands of Raman scattering are superimposed on a wide band of NDs fluorescence. It should be mentioned that while Raman spectra contain the fluorescence band of NDs, due to the low concentration of nanoparticles the Raman signal from their surface groups does not contribute to the overall spectra (see the “0 mM” line on the Fig. 2a). In all, three spectral ranges of Raman scattering are of

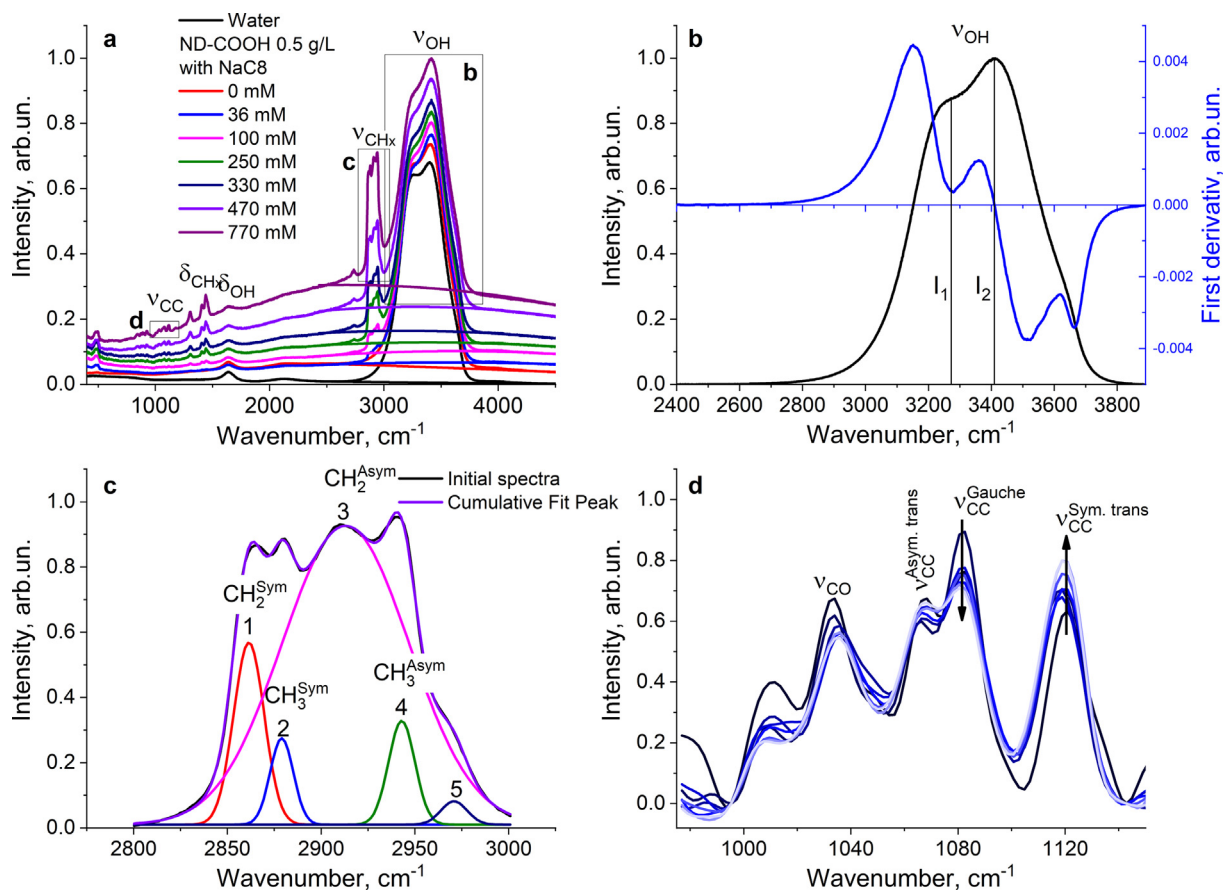


Fig. 2. Raman scattering spectra of water and aqueous suspensions of ND-COOH with a concentration of 0.5 g/L at different concentrations of NaC8 (a). Illustration of χ_{21} parameter calculations (b). An example of the decomposition of bands of stretching vibrations of CH_x -groups into 5 components of a Gaussian shape (c). The Raman spectrum region of stretching vibrations of C–C groups measured at concentrations from 100 to 1500 mM of NaC8 in aqueous suspensions of ND-H. Arrows denote the increase of NaC8 concentration (d).

interest in the analysis of molecular interactions in aqueous suspensions: the region of stretching vibrations of water molecules (Fig. 2b), the stretching vibrations region of CH-groups (Fig. 2c) and the region of “skeletal” vibrations of the C–C bond of the hydrocarbon tail (Fig. 2d).

3.3. The parameters used to characterize the spectral bands

To quantify the changes in the Raman spectra and related changes of properties of studied suspensions, four parameters – χ_{21} , η/ξ , ψ , δ – were used.

The parameter χ_{21} . As follows from the obtained data, the water stretching band ν_{OH} (Fig. 2a) undergoes significant changes with increasing surfactant concentration: the intensity of the high-frequency region of the stretching band increases, whereas the intensity of the low-frequency region decreases, and the band itself shifts toward higher frequencies. Majority of authors [44–48] assign the low-frequency region of the stretching band to OH vibrations with strong hydrogen bonds and the high-frequency region to OH vibrations with weak hydrogen bonds. Therefore, the redistribution of intensity between the high-frequency and low-frequency regions of the band is caused by the strengthening or weakening of hydrogen bonds in a solution [44–48]. To quantify the change in the strength of the hydrogen bonds, the parameter χ_{21} , which is equal to the ratio of the intensities of

high-frequency (I_2) and low-frequency (I_1) regions of the stretching band of OH groups (Fig. 2b) was introduced [46,47]. To distinguish the stretching band of OH groups from ND's fluorescence, the last was approximated by a second-degree polynomial and subtracted from the spectrum (Fig. 2a). Frequencies 1 and 2 were determined from the singular points of the stretching band derivative (Fig. 2b). The obtained dependences $\chi_{21}(C_{\text{NaC8}})$ are presented in Fig. 3a. As it follows from the definition of the parameter, an increase in the parameter χ_{21} means a weakening of hydrogen bond strength in aqueous media.

Decomposition of the band of CH stretching vibrations. As indicated above, the stretching vibration bands ν_{CH_x} of CH-groups in the 2800–3100 cm^{-1} region are sensitive to structural changes of NaC8 molecules and their local environment [39–41]. There are bands of symmetric (2865 cm^{-1}) and antisymmetric (2915 cm^{-1}) vibrations of CH bonds in CH_2 -groups, and also symmetric (2885 cm^{-1}) and antisymmetric (2945 cm^{-1}) vibrations of CH bonds in CH_3 -groups (Fig. 2a, b) [49]. With the increase of the NaC8 concentration in suspensions, the position of individual vibrations shifts to the lower frequencies without changes in the overall shape of the spectrum. To prevent confusion, from here onwards we will call the CH bands not by their position but by their assignments, with the full band named as CH_x .

To extract these vibration bands, the regions of 2800–3000 cm^{-1} of Raman spectra of all samples were decomposed into

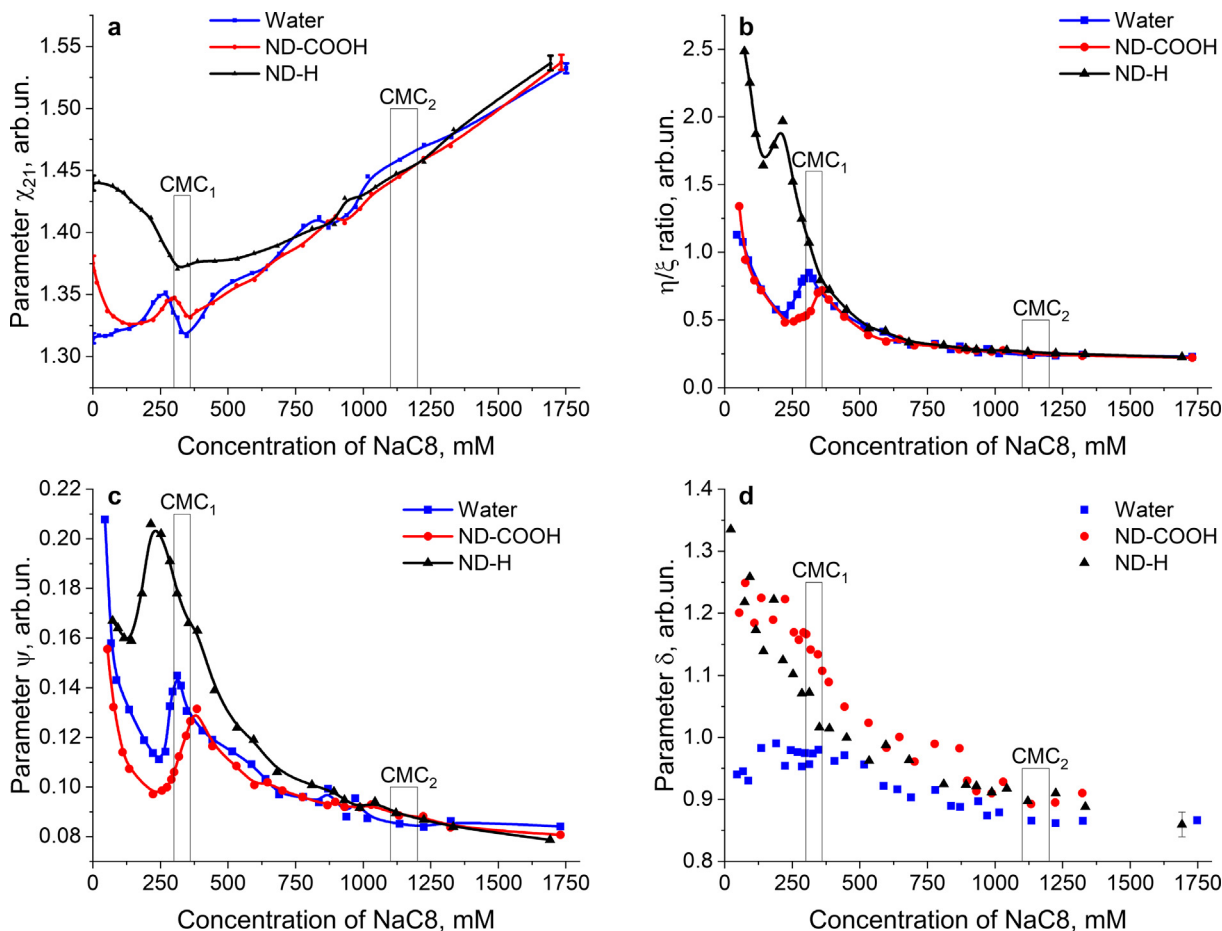


Fig. 3. Dependencies of the parameters χ_{21} corresponding to the strength of hydrogen bonds (a) [34] ©Nanosystems: Physics, Chemistry, Mathematics, St. Petersburg National Research University of Information Technologies, Mechanics and Optics, η/ξ corresponding to the ordering of hydrocarbon tails of NaC8 (b), ψ corresponding to the polarity of the environment of NaC8 tails (c), and δ corresponding to the ratio of C–C bonds with “gauche” and “trans” isomerism in suspensions (d) on the concentration of sodium octanoate in water and aqueous suspensions of ND-COOH and ND-H. The depicted ranges of the CMCs represent the CMCs range according to the literature data for the aqueous solutions of NaC8, without dispersed NDs. Error bars denote the experimental errors that were substantially higher than the difference between the values of studied parameters in three repeats of the experiment. Experimental errors in b and c are 0.01 arb.un. and 0.002 arb.un., respectively, and are overcast by plotted dots.

five Gaussian contours using the Levenberg-Marquardt algorithm by Origin. The results of the decomposition of one of the obtained spectra are shown in Fig. 2c. The first and the third components correspond to symmetric and antisymmetric vibrations of CH groups in CH₂, the second and the fourth – to symmetric and antisymmetric vibrations of CH groups in CH₃, respectively. The fifth component (a shoulder in the region of 2975 cm⁻¹) is possibly due to the Fermi resonance between the stretching vibrations and overtones of deformation vibrations of CH-groups [50].

The parameter η/ξ . To analyze the ordering of hydrocarbon tails of surfactants in samples, the ratio of the integral intensity η of the band of symmetric stretching vibrations of CH₂ (CH₂^{sym}) to the integral intensity ξ of the band of symmetric stretching vibration of CH₃ (CH₃^{sym}), the parameter η/ξ , was used [39,41]. The integral intensity of the bands of symmetric vibrations of CH in CH₂ groups was calculated as the ratio of the area of the Gaussian contour corresponding to these oscillations to the sum of the areas of the contours corresponding to symmetric and antisymmetric CH oscillations in CH₂ groups: $\eta = S_{CH_2}^{sym} / (S_{CH_2}^{sym} + S_{CH_2}^{asym})$. Similarly for the CH band in CH₃-groups: $\xi = S_{CH_3}^{sym} / (S_{CH_3}^{sym} + S_{CH_3}^{asym})$. The normalization to the sum of the areas of the contours was carried out to exclude the influence of instrumentation factors (changes in scattering due to inhomogeneity of media). The obtained dependences η/ξ (C_{NaC8}) are presented in Fig. 3b. A decrease in the parameter η/ξ means an increase in the ordering of hydrocarbon tails of NaC8 in the suspension.

The parameter ψ . According to Larsson and Rand [39], the intensity of the band of asymmetric stretching vibration of CH₃ (CH₃^{asym}) is correlated with the polarity of the environment or, in this case, to the number of water molecules around the hydrocarbon tails. Therefore, to characterize the changes in the polarity of the environment of NaC8 hydrocarbon tails in studied samples, the relative integral intensity of asymmetric oscillations of CH in CH₃ groups, the parameter $\psi = S_{CH_3}^{asym} / S_{CH_3}$, was used. The obtained dependences ψ (C_{NaC8}) are presented in Fig. 3c. A decrease in the parameter ψ means a decrease of the polarity of the environment of NaC8 tail and thus a decrease of a number of water molecules in its immediate vicinity.

The parameter δ . In the region of 1000–1150 cm⁻¹ of the Raman spectrum of surfactant solutions, there are bands ν_{CC} of C–C stretching vibrations of hydrocarbon tails (Fig. 2d). The band with a maximum at 1078 cm⁻¹ corresponds to C–C vibrations with “gauche” isomerism, when bands with maxima at 1066 cm⁻¹ and 1125 cm⁻¹ – to C–C vibrations with “trans” isomerism [40,42]. Thus, the parameter $\delta = I_{1078} / I_{1125}$ (where I is a peak intensity) reflects the ratio of C–C bonds with “gauche” and “trans” isomerism. The obtained dependences δ (C_{NaC8}) are presented in Fig. 3d. A decrease in the parameter δ means a transformation of gauche-isomers of segments of hydrocarbon tails to trans-isomers.

The values of four parameters – χ_{21} , η/ξ , ψ , δ – were calculated for the Raman spectra of water and aqueous suspensions of hydrophobic and hydrophilic nanodiamonds at increasing NaC8 concentrations and plotted in Fig. 3. These four parameters correspond to the strength of hydrogen bonds, to the ordering of hydrocarbon tails of NaC8, to the polarity of the environment of NaC8 tails, and to the ratio of C–C bonds with “gauche” and “trans” isomerism in suspensions, accordingly. The part of our results (considering the χ_{21} parameter and elucidated shielding of hydrogen bonds from the weakening influence of NDs by the NaC8, about which will be discussed further) was already presented in our previous short manuscript [34]. Due to the great importance for the formation and understanding of the model of studied processes, we repeated experiments from [34] achieving greater accuracy and presented them here.

Before analyzing the results, we note that in water the sodium octanoate dissociates onto the Na⁺ ion and the octanoate anion often called simply octanoate, a carboxylate ion with a hydrocarbon tail. Both ions interact with water molecules surrounding them and are always present in the solution. Hydrated ions change the structure of water, which is manifested in a change of the characteristics of the water stretching band [47,48]. However, the influence of Na⁺ cations on the water’s structure is rather small [47,48], therefore the Raman spectra are weakly changed. Thus, we assume that changes in the water stretching band are caused primarily by interactions of the nanodiamonds and octanoate anions with water molecules, and the influence of Na⁺ ion can be neglected.

3.4. Influence of NDs and surfactant interactions on water properties and micelle formation

From the obtained data (Fig. 3), it can be seen that all four parameters – characteristics of the strength of the hydrogen bonds (χ_{21}), the ordering of hydrocarbon tails of NaC8 (η/ξ), the polarity of the environment of NaC8 tails (ψ), and the ratio of C–C bonds with “gauche” and “trans” isomerism (δ) – change with NaC8 concentration in all suspensions. It should be noted that the notable alterations of the obtained dependences of all four parameters on C_{NaC8} occur mainly in the region around CMC₁. Additionally, for different samples these changes occur mainly in a similar way, but in different intensities and positions. The dependences of χ_{21} , η/ξ , and ψ parameters on the concentration of NaC8 are generally the same for water and aqueous suspension of hydrophilic ND-COOH but differ for aqueous suspension of hydrophobic ND-H. In case of the parameter δ , its dependence on C_{NaC8} for the water differs from those for the suspensions of both hydrophilic and hydrophobic nanodiamonds.

The behavior of the χ_{21} , η/ξ , ψ , δ parameters and, consequently, the changes in the suspensions they represent, can be divided into three different regions of NaC8 concentration: low concentrations before CMC₁, micelle formation region, and high concentrations of NaC8. The discussion below is mainly structured correspondingly, using the schematic representations of ND - NaC8 interactions from Fig. 4, and starting with the suspension without NaC8.

3.4.1. In the absence of sodium octanoate

In the absence of sodium octanoate (C_{NaC8} = 0 mM) the values of parameter χ_{21} for both ND suspensions are much higher than that for water, and, subsequently, the hydrogen bonds are much weaker in both ND suspensions than in water. Moreover, hydrogen bonds are weaker in suspensions of hydrophobic nanodiamonds than in suspensions of hydrophilic NDs (Fig. 3a), even taking into account that the concentration of ND-H in the suspension is half of ND-COOH.

We believe that the weakening of hydrogen bonds in the first place is caused by micro-flows of the fluid induced by Brownian motions of the nanoparticles. Such micro-flows are hard to be detected, but it was theorized that they, among other possible manifestations, are responsible for the enhancement of thermal conductivity [51] and of mass transport [52] in nanofluids.

Then, ND-H nanoparticles in water loosen the network of hydrogen bonds more strongly in comparison to ND-COOH because of its hydrophobicity (including zeta potential positivity, Fig. 1), i.e. due to the repulsion of water molecules from the ND-H surface (Fig. 4d–f) [32].

3.4.2. At low concentrations of sodium octanoate (C_{NaC8} < CMC₁)

When adding a surfactant in the suspension, another factor besides NDs begins to affect the hydrogen bonds. Propagating

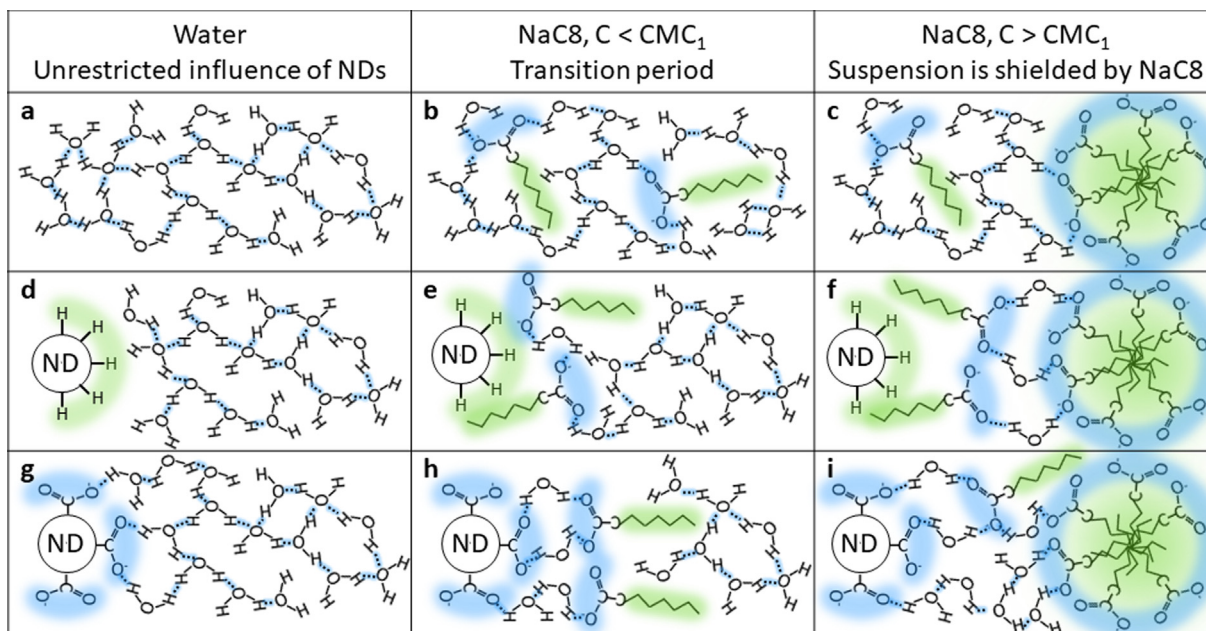


Fig. 4. Schematic representations of interactions in aqueous suspensions of hydrophobic and hydrophilic nanodiamonds and sodium octanoate.

throughout the entire volume (the number of NaC8 molecules at 100 mM concentration is already hundreds of thousands of times larger than the number of ND particles in the suspensions), NaC8 molecules are embedded between water molecules and nanodiamonds, creating a certain structure and changing the distribution of hydrogen bond forces. In water without NDs, a gradual weakening of hydrogen bonds is observed due to the hydrophobic hydration of NaC8 molecules (Fig. 3a).

The state of the NaC8 molecules in water can be analyzed using the parameters η/ξ , ψ , and δ . At the first points of their dependences on NaC8 concentration (Fig. 3b–d), NaC8 molecules are represented only by monomers surrounded solely by water molecules and occasional NDs. In this state, the disorder of NaC8 hydrocarbon tails (η/ξ) and the number of water molecules in their vicinity (ψ) are the highest (Fig. 3b, c). With the increasing concentration of NaC8, its molecules begin to form dimers. This process results in the ordering of hydrocarbon tails (decrease of η/ξ value) and in the decrease of the number of water molecules in their vicinity (decrease of ψ value) (Fig. 3b,c). However, such interactions do not influence the relative number of gauche- and trans-isomers in suspensions – the value of the parameter δ at premicellar concentrations in water stays relatively the same.

In the suspensions of NDs, the state of NaC8 molecules undergoes changes. At the same concentrations of NaC8 below CMC_1 , the disorder of tails (η/ξ) and the polarity of their environment (ψ) are substantially higher in the presence of hydrophobic NDs than that in pure water (Fig. 3b,c). The presence of hydrophilic NDs does not influence the order of NaC8 tails but slightly reduces the polarity of NaC8 environment (Fig. 3b,c). Specific behavior of NaC8 in the presence of ND-H is explained by the duality of interactions of NaC8 molecules and hydrophobic surface of these NDs: (1) the surface of ND-H is positively charged, which ensures the attraction of a negatively charged surfactant head (Fig. 4e), (2) at the same time the nearby placement of hydrophobic parts – ND-H surfaces and hydrocarbon octanoate tail (Fig. 4e) – is also energetically favorable [49]. This “dual” interaction and dense arrangement of NaC8 molecules near the ND-H surface provide the disorder of surfactant tails (the higher values of the parameter η/ξ) which in turn increases the number of water molecules in their vicinity (the higher values of the parameter ψ) (Fig. 3b, c).

It should be noted that the difference in interactions between surfactants and hydrophobic/hydrophilic nanodiamonds does not influence the isomerism of NaC8 tails: at $C_{NaC8} < CMC_1$ the dependences $\delta(C_{NaC8})$ are similar for both suspensions of NDs and differ from that for water (Fig. 3d). The values of the parameter δ for suspensions of both NDs are higher than that for water, what means that in the suspensions of NDs the tails of NaC8 are more “twisted” – the relative number of their gauche-isomers is greater – compared to the tails of NaC8 in water. The similarity in the dependences $\delta(C_{NaC8})$ for different NDs indicates that the NaC8 isomerism is mostly independent on the hydrophilicity of NDs surface, although the presence of nanoparticles significantly affects it. We attribute this influence (that is slightly stronger for the suspensions of ND-COOH) to the aforementioned induction of microflows in the suspensions by the Brownian motions of diffused NDs, which is more intensive for the ND-COOH due to their higher concentrations and smaller sizes (0.5 g/L of 12 nm ND-COOH against 0.25 g/L of 24 nm ND-H). However, with the increase of NaC8 concentration, the molecules of NaC8 stabilize the suspensions and shield the bulk of molecules from the influence of NDs – the parameter δ decreases.

The shielding of the suspensions by NaC8 molecules from the influence of NDs is also observed through the changes of the parameter χ_{21} (Fig. 3a). For the suspension of hydrophilic NDs the strength of hydrogen bonds abruptly increases (the parameter χ_{21} abruptly decreases) to the level of those in water at NaC8 concentrations about 100 mM – significantly below CMC_1 . In a suspension of hydrophobic nanodiamonds, in contrast to water and suspension of hydrophilic nanodiamonds, the parameter χ_{21} gradually decreases with increase in the concentration of NaC8 molecules up to $C_{NaC8} = 330$ mM, i.e. hydrogen bonds gradually become stronger. At the same time, at NaC8 concentration up to 500–600 mM, the hydrogen bonds are weaker in this suspension than in the other two samples (Fig. 3a). Both effects of strengthening of hydrogen bonds in NDs suspensions with the addition of NaC8 can be explained by the surfactant screening the influence of NDs on water molecules. However, the “dual” interaction of ND-H with positively charged hydrophobic surface and NaC8 with negatively charged head and hydrophobic tail ensures gradual screening without a formation of uniform and effective “shield”

of NaC8 molecules up to $C_{\text{NaC8}} = 330$ mM. For ND-COOH, direct interaction of their surface groups with the octanoate is impossible, octanoate ions interact with them only through the shell of the water molecule (Fig. 4h). However, this double shell of water molecules and anions of NaC8 effectively screen the effect of ND-COOH on hydrogen bonds of water molecules starting from a low concentration of surfactants (Fig. 3a). Part of the shielding effect can be attributed to the increase of the viscosity in the NaC8 suspensions and consequent decrease in the intensity of NDs' Brownian motions. However, the quantification of viscosity's exact contribution is a separate complex task.

3.4.3. Micelle formation region

In the NaC8 concentration region immediately before, during ($C_{\text{NaC8}} = \text{CMC}_1$) and after micelle formation, qualitative changes are observed in the dependences of all studied parameters: $\chi_{21}(C_{\text{NaC8}})$, $\eta/\xi(C_{\text{NaC8}})$, $\psi(C_{\text{NaC8}})$, $\delta(C_{\text{NaC8}})$ (Fig. 3). In the dependencies of $\eta/\xi(C_{\text{NaC8}})$ and $\psi(C_{\text{NaC8}})$ characterizing the order of surfactant tails and the number of water molecules in their vicinity, there are sharp peaks. The dependence of the parameter $\delta(C_{\text{NaC8}})$, characterizing the ratio of gauche- to trans-isomers in NaC8 tail, in water turns from the constant to the decreasing. In the dependencies of the parameter $\chi_{21}(C_{\text{NaC8}})$, characterizing the strength of hydrogen bonds in suspensions, for water and hydrophilic ND-COOH the "sinusoid" trend is observed, while the dependence of parameter $\chi_{21}(C_{\text{NaC8}})$ for hydrophobic ND-H turns from decreasing to increasing.

All observed changes and, in particular, the peaks in the dependences of the parameters $\eta/\xi(C_{\text{NaC8}})$ and $\psi(C_{\text{NaC8}})$ are explained by the restructuring of the NaC8 tails through dimers decomposition and by the following structuring through micelle formation. Dimer decomposition leads to the sharp increase of a number of water molecules in the close vicinity of hydrocarbon tails and disorder of the surfactants, while the following micelle formation reverses the process: order of NaC8 tails increases (decrease of the parameter η/ξ) and number of water molecules around NaC8 tail decreases (decrease of the parameter ψ). The position of the peaks in the dependences of parameters $\eta/\xi(C_{\text{NaC8}})$ and $\psi(C_{\text{NaC8}})$ can be interpreted as the NaC8 concentration at which the micelles begin to form – as the critical micelle concentration (CMC_1). According to our results, this concentration for the aqueous solution of NaC8 lies at 310 mM within the range of 300–360 mM determined using different experimental methods [37]. Using the measured positions of peaks in the dependencies of the parameters $\eta/\xi(C_{\text{NaC8}})$ and $\psi(C_{\text{NaC8}})$ for NDs suspensions, it was determined that the presence of hydrophobic ND-H with the concentration 0.25 g/L shifts the value of CMC_1 on 90–150 mM to lower concentrations and the presence of hydrophilic ND-COOH with the concentration 0.5 g/L shifts the value of CMC_1 on 40–50 mM to higher concentrations in comparison to the value of CMC_1 in water without NDs.

The earlier micelle formation in the presence of ND-H results from the chaotic state of NaC8 in this suspension caused by the "dual" interactions of NaC8 with the ND-H. In this chaotic state octanoate tails are highly disordered (high values of the parameter η/ξ , Fig. 3b), they are mainly surrounded by water (high values of the parameter ψ , Fig. 3c), while they can move more freely due to the lower strength of hydrogen bonds (high values of the parameter χ_{21} , Fig. 3a). In result of this disorder of NaC8 molecules (small number of dimers) and more freedom of movements, the NaC8 molecules begin to form micelles at NaC8 concentration lower than CMC_1 in water without hydrophobic NDs.

While in general hydrophilic ND-COOH do not create a 'chaos' in the suspensions of NaC8, they nonetheless induce the micro-flows in the suspensions due to their Brownian motions (which results in the increase of a number of NaC8 tails in gauche-isomers, the higher values of the parameter δ , Fig. 3d). Apparently,

such micro-flows inhibit the formation of stable conglomerates of NaC8 – micelles, which leads to the increase of CMC_1 on 40–50 mM. Undoubtedly, the induction of micro-flows plays role in the suspensions of ND-H too, however, the described chaotic state of these suspensions nevertheless ensures the formation of micelles at lower NaC8 concentrations.

The dimer decomposition and the following micelle formation influence the strengths of hydrogen bonds in suspensions: the dependencies of $\chi_{21}(C_{\text{NaC8}})$ deviate from monotonic growth in the sinusoid form for water and ND-COOH suspension, while relatively at the same NaC8 concentration the shoulder in the dependence of $\chi_{21}(C_{\text{NaC8}})$ for ND-H occurs (Fig. 3a). In the range of $C_{\text{NaC8}} = 240\text{--}300$ mM dimers became to decompose in the monomers what leads to the overall decrease of strength of hydrogen bonds in suspensions characterized by an increase in the χ_{21} value. Following micelle formation ensures that a large part of the NaC8 tails interact in general with other NaC8 tails and not with the water environment – the parameter χ_{21} decreases. The subsequent increase of a number of NaC8 molecules increases the number of micelles as well as occasional monomers and dimers, what results in the gradual decrease of hydrogen bonds strength. The Raman scattering technique makes it possible to "feel" the transition to micelle formation: the χ_{21} values became sinusoidal [43] (Fig. 3a). In the presence of hydrophilic nanodiamonds, the amplitude of this sinusoid is smaller, it is observed at larger C_{NaC8} and the sinusoid period is shorter compared with this of $\chi_{21}(C_{\text{NaC8}})$ in water. This means that the formation of micelles in the ND-COOH suspension is more difficult compared with micelle formation in water, although the hydrogen bonds in these two samples in the region of the CMC_1 are almost the same (Fig. 3a). The micelle formation of surfactant in ND-COOH suspensions is hampered by Brownian motion and diffusion of nanodiamonds. For hydrophobic NDs a shoulder is observed in the dependence of $\chi_{21}(C_{\text{NaC8}})$ at a lower concentration, than a "sinusoid" in water and in the ND-COOH suspension. At that moment, the duality of interactions between ND-H and surfactant disappears and the hydrophobic interaction becomes dominant (Fig. 4f). As it was mentioned, the significant weakening of hydrogen bonds in aqueous suspensions of ND-H facilitate the faster and easier formation of micelles in this sample as compared to the other two samples, even taking into account the Brownian motion and diffusion of nanodiamonds in both suspensions.

3.4.4. At high concentrations of sodium octanoate ($C_{\text{NaC8}} > \text{CMC}_1$)

At the points of NaC8 concentrations higher CMC_1 , four studied parameters resume to change in the same way as at the points prior to CMC_1 . These changes correspond to the structuring of the surfactants, now into micelles. The difference in the tendencies of the dependences between the regions prior and after the CMC_1 occur in the dependence $\delta(C_{\text{NaC8}})$ for NaC8 aqueous solution. As follows from Fig. 3d, the relative number of molecules with "gauche" isomerism for this solution is practically constant at $C_{\text{NaC8}} < \text{CMC}_1$, then decreases with increasing surfactant concentration. The location of the NaC8 molecules in the micelles "straightens" them, making it unfavorable for the tail to remain in the "gauche" conformation. These results are in full agreement with the previous studies [53–55].

With increasing of the concentration of NaC8 from CMC_1 and above, the differences between all studied suspensions in the dependencies of all four parameters $\chi_{21}(C_{\text{NaC8}})$, $\eta/\xi(C_{\text{NaC8}})$, $\psi(C_{\text{NaC8}})$, $\delta(C_{\text{NaC8}})$ decreases and after some point practically nullifies (Fig. 3), i.e. the hydrogen bonds, the order of NaC8 tails, the polarity of their environment and their isomerism change monotonically in the same way for all studied samples. At first, it occurs due to the screening of the influences of both types of NDs by surfactant and formation of micelles on which NDs can't exert the

great influence (Fig. 4f,i). With the further increase of the concentrations of NaC8, the overall impact of NDs on the environment decreases compared to the structure defined by surfactants. At NaC8 concentrations higher CMC_2 the hydrogen bonds continue to weaken, while the changes in the studied properties of octanoate ions, according to the dependencies η/ξ $\xi(C_{NaC8})$, $\psi(C_{NaC8})$, $\delta(C_{NaC8})$, practically disappear.

The described changes in the suspensions of nanodiamonds are illustrated in Fig. 4.

Thus, at low concentrations of NaC8 the network of hydrogen bonds and the course of micelle formation in suspensions change significantly. These changes depend on the type of functional surface groups of nanoparticles. The more NDs weaken the hydrogen bonds in aqueous surfactant solutions, the faster and easier the micelle formation takes place in the medium. In the presence of NDs with hydrophobic surface groups in aqueous solutions of surfactants, hydrogen bonds are significantly weakened compared to those in the suspensions of NDs with hydrophilic groups and in water, which facilitates the faster formation of micelles. On the other hand, Brownian motion and diffusion of nanodiamonds slightly inhibit micelle formation. Thus, the corresponding functionalization of the ND surface can be used to control the course of micelle formation in media.

It should be noted that, in contrast to the behavior of the functions η/ξ $\xi(C_{NaC8})$ and $\psi(C_{NaC8})$ for the bands of vibrations of CH groups, the dependences of the fraction of hydrocarbon tails with “gauche” conformation on the surfactant concentration $\delta(C_{NaC8})$ are similar for the suspensions of both nanodiamonds and differ from $\delta(C_{NaC8})$ for aqueous solutions of NaC8. This indicates that although hydrophilic nanodiamonds do not interact directly with hydrocarbon tails, their influence on the surrounding molecules extends far enough, which agrees with the literature data [28,29].

Therefore, by the means of the Raman spectroscopy and dynamic light scattering technique the nano-scale effects of nanodiamonds on the surfactants – the close relative of amphiphilic lipids, and their micelles, were studied. The results of this research allowed us to distinguish two different mechanisms by which NDs change the structure of the suspensions of surfactants, as well as their effects. Our findings can bring light to the nano-effects of nanoparticles on biological tissues, while simultaneously from the new side affirm the biocompatibility and safety of nanodiamonds for the solutions of structured supramolecules.

4. Conclusions

In this work, the interactions of hydrophobic (ND-H) and hydrophilic (ND-COOH) nanodiamonds with the molecules of water suspensions of surfactant (sodium octanoate, NaC8) – the simplest model of biological tissues – were studied. The emphasis of the previous studies of interactions of NDs and surfactants was on the improvement of colloidal properties of nanoparticles under the influence of surfactants [22–25]. This paper is the first to explore the other side of these interactions – the influence of NDs on the nanoscale properties of surfactant solutions – the subject of the extreme importance for ensuring the safety and biocompatibility of nanoparticles used as photoluminescent markers and drug carriers. Employed methods of Raman spectroscopy and dynamic light scattering allowed to reveal the significant changes in surfactant properties caused by the interactions of the NDs, surfactant molecules, and water in suspensions, tracked through the large range of NaC8 concentrations from 0 to 1700 mM, corresponding to the premicellar state, the micelle formation zone (CMC zone around 330 mM) and the surfactant solution with the formed micelles.

It was found that only in the premicellar region NDs exhibit a significant influence on the bulk properties of surfactant solutions. It is shown that NDs of both types, hydrophobic and hydrophilic, weaken the strength of hydrogen bonds in water, what corresponds with our previous findings [30–32]. However, the surfactant was found to screen such an effect of NDs: effectively for ND-COOH and only gradually reducing their weakening influence up to the CMC region for ND-H. At the same time, negatively charged ND-COOH are found to have almost no effect on the ionic surfactant, while positively charged ND-H are found to significantly change surfactant properties in the premicellar region. It is concluded that ND-H generates a “chaotic” state of the NaC8 solution around them: they actively weaken the hydrogen bonds of their environment and disorder the hydrocarbon tails of surfactants, which leads to the effective destruction of the premicellar structures. This effect is explained by the “dual” interaction of hydrophobic NDs and ionic surfactant: a combination of hydrophobic interaction of the NDs’ surface and the surfactant tails, and the Coulomb attraction of the surfactant head to the positively charged NDs’ surface. Easy to imagine, the existence of such an interaction is experimentally proved for the first time in this paper, while its effect on the bulk properties of the molecules surrounding NDs was investigated.

Moreover, both types of NDs are found to equally “bend” the surfactant tails: the ratio of the number of surfactant tails in the gauche conformation to the number of tails in the trans conformation in the presence of NDs significantly increases. These changes in the conformation of surfactant tails are caused by the induction of the micro-flows in the vicinity of NDs, that originates from the Brownian motions of NDs while almost independent on the surface type of NDs. Before, the effect of such micro-flows was shown only for the enhancement of thermal conductivity [51] and of mass transport [52] in nanofluids.

Two discovered mechanisms of the NDs’ influence – the induction of micro-flows in the fluid independent on the particular surface of NDs and the creation of “chaotic” state of the surfactant solutions around the ND-H caused by their “dual” interactions with the ionic surfactant – explain the established changes of CMC_1 value of NaC8 in the presence of NDs. The ND-induced micro-flows in the suspensions inhibit the formation of lasting structures and shift the value of CMC_1 to the bigger concentrations, while the chaotic state of the suspensions characteristic to the ND-H ensures the freer movements of surfactants responsible for a creation of the micelles at the concentrations lower than CMC_1 in water without hydrophobic NDs. Like that, in the presence of 0.25 g/L of hydrophobic ND-H (0.5 g/L of hydrophilic ND-COOH), the micelle formation occurs at surfactant concentrations of 90–150 mM less (40–50 mM more) than CMC_1 in water without NDs. Due to the assumption of even distribution of NDs and the prevailing number of NaC8 molecules it is expected that the shifts of CMC_1 will be enhanced up to some limits with the increase of the concentration of NDs in the suspensions and diminished with the decrease of NDs number. Thus, the possibility of controlling the micelle formation by means of ND functionalization was demonstrated.

At the presence of NaC8 at concentrations higher CMC_1 , the structure of the surfactant-NDs suspensions is found to be defined solely by the growing micelles while all influence of NDs disappeared. These results allow us to conclude that in the biological environment with formed micelles NDs of both types do not destroy the surrounding micellar structures.

The found mechanisms of NDs’ influence on the surfactant molecules are believed to diminish when the NDs’ concentration decreases, and not fundamentally change when surfactants are exchanged by ones with longer hydrocarbon tails or with a different hydrophilic-lipophilic balance (HLB). For these surfactants, NDs are believed to nonetheless exert significant effect only on the non-

micellized surfactant solutions: to induce the micro-flows in the suspensions and, as a result, to bend the surfactants tails, and to destabilize the surfactant solutions if the two incompatible variants of the interactions between ND's surfaces and surfactants are similarly favorable. Moreover, the proposed mechanisms of NDs' influence occur to be non-specific for NDs or even carbon nanoparticles. We expect the occurrence of the effects, similar to observed for NDs, for all nanoparticles with defined surface charges and hydrophobicity. However, the verification of this hypothesis we leave to the future studies.

Thus, the present study sheds light on the features and mechanisms of the interaction of nanodiamonds and surfactants in aqueous suspensions and can be a starting point in studies of their interactions in complex biological environments.

Acknowledgments

Fundings: This work was supported by the Russian Science Foundation [grant number 17-12-01481] (S.A.B., K.A.L., T.A.D. – planning and conducting of the experiment, discussion of results), was partially supported by the Russian Foundation for Basic Research [grant number 18-32-00779 mol_a] (A.M.V. – conducting of the experiment, analysis and discussion of results) and was partially supported by MPEH Academic Excellence Project 02. a03.21.0005, 27.08 (I.I.V. – discussion of results). The authors are sincerely grateful to T. Petit, J.-Ch. Arnault and H.A. Girard for providing an aqueous suspension of ND-H, and J.M. Rosenholm for providing the opportunity to conduct measurements using the Malvern ZetaSizer.

Appendix A. Supplementary material

Supplementary data to this article can be found online at <https://doi.org/10.1016/j.jcis.2019.03.102>.

References

- [1] K. Turcheniuk, V.N. Mochalin, Biomedical applications of nanodiamond (review), *Nanotechnology* 252001 (28) (2017) 1–28, <https://doi.org/10.1088/1361-6528/aa6ae4>.
- [2] J.M. Rosenholm, I.I. Vlasov, S.A. Burikov, T.A. Dolenko, O.A. Shenderova, Nanodiamond-based composite structures for biomedical imaging and drug delivery (review), *J. Nanosci. Nanotechnol.* 15 (2015) 959–971, <https://doi.org/10.1166/jnn.2015.9742>.
- [3] M. Chen, E.D. Pierstorff, R. Lam, S.Y. Li, H. Huang, E. Osawa, D. Ho, Nanodiamond-mediated delivery of water-insoluble therapeutics, *ACS Nano* 3 (7) (2009) 2016–2022, <https://doi.org/10.1021/nn900480m>.
- [4] K.K. Liu, W.W. Zheng, C.C. Wang, Y.C. Chiu, C.L. Cheng, Y.S. Lo, C. Chen, J.I. Chao, Covalent linkage of nanodiamond-paclitaxel for drug delivery and cancer therapy, *Nanotechnology* 21 (2010) 315106, <https://doi.org/10.1088/0957-4484/21/31/315106>.
- [5] R. Lam, D. Ho, Nanodiamonds as vehicles for systemic and localized drug delivery, *Expert Opin. Drug Deliv.* 6 (9) (2009) 883–895, <https://doi.org/10.1517/17425240903156382>.
- [6] L.-C.L. Huang, H.-C. Chang, Adsorption and immobilization of cytochrome C on nanodiamonds, *Langmuir* 20 (14) (2004) 5879–5884, <https://doi.org/10.1021/la0495736>.
- [7] T.A. Dolenko, S.A. Burikov, K.A. Laptinskii, T.V. Laptinskaya, J.M. Rosenholm, A. A. Shiryayev, A.R. Sabirov, I.I. Vlasov, Study of adsorption properties of functionalized nanodiamonds in aqueous solutions of metal salts using optical spectroscopy, *J. Alloys Compd.* 586 (2014) S436–S439, <https://doi.org/10.1016/j.jallcom.2013.01.055>.
- [8] E. Perevedentseva, P.-J. Cai, Y.-C. Chiu, C.-L. Cheng, Characterizing protein activities on the lysozyme and nanodiamond complex prepared for bio applications, *Langmuir* 27 (3) (2011) 1085–1091, <https://doi.org/10.1021/la103155c>.
- [9] X. Wang, X.C. Low, W. Hou, L.N. Abdullah, T.B. Toh, M. Mohd Abdul Rashid, D. Ho, E.K.-H. Chow, Epirubicin-adsorbed nanodiamonds kill chemoresistant hepatic cancer stem cells, *ACS Nano* 8 (2014) 12151–12166, <https://doi.org/10.1021/nn503491e>.
- [10] D. Ho, Nanodiamond Modified Gutta Percha (NDGP) Composite for Non-Surgical Root Canal Therapy (RCT) Filler Material Applied by Vertical Condensation Obturation Procedure, University of California, Los Angeles, 2016.
- [11] B. Alberts, A. Johnson, J. Lewis, M. Raff, K. Roberts, P. Walter, *Molecular Biology of the Cell*, fifth ed., Garland Science, New York, 2007.
- [12] J.N. Israelachvili, *Intermolecular and Surface Forces*, second ed., Academic Press Harcourt Brace & Company, London, 1992.
- [13] R. Nagarajan, One Hundred Years of Micelles: Evolution of the Theory of Micellization, in: L. Romsted (Ed.), *Surfactant Science and Technology: Retrospects and Prospects*, Taylor and Francis, New York, 2013, pp. 3–52.
- [14] Yu.A. Mirgorod, T.A. Dolenko, Liquid polyamorphous transition and self-organization in aqueous solutions of ionic surfactants, *Langmuir* 31 (31) (2015) 8535–8547, <https://doi.org/10.1021/acs.langmuir.5b00479>.
- [15] M.-A. Ahmadi, Z. Ahmad, L.T.K. Phung, T. Kashiwao, A. Bahadori, Experimental investigation the effect of nanoparticles on micellization behavior of a surfactant: application to EOR, *Petrol. Sci. Technol.* 34 (2016) 1055–1061, <https://doi.org/10.1080/10916466.2016.1148051>.
- [16] J. Jin, X. Li, J. Geng, D. Jing, Insights into the complex interaction between hydrophilic nanoparticles and ionic surfactants at the liquid/air interface, *Phys. Chem. Chem. Phys.* 20 (2018) 15223–15235, <https://doi.org/10.1039/c8cp01838c>.
- [17] O.A. Soboleva, M.G. Chernysheva, I.Y. Myasnikov, V.A. Kostin, G.A. Badun, Effect of Pluronic P123 on the distribution of nanodiamond particles in water-organic liquid systems, *Russ. J. Phys. Chem. A* 91 (2017) 130–135, <https://doi.org/10.1134/S0036024417010265>.
- [18] X. Zhang, S. Wang, M. Liu, J. Hui, B. Yang, L. Tao, Y. Wei, Surfactant-dispersed nanodiamond: biocompatibility evaluation and drug delivery applications, *Toxicol. Res.* 2 (5) (2013) 335–342, <https://doi.org/10.1039/c3tx50021g>.
- [19] R.A. Sperling, W.J. Parak, Surface modification, functionalization and bioconjugation of colloidal inorganic nanoparticles, *Phil. Trans. R. Soc. A* 368 (2010) 1333–1383, <https://doi.org/10.1098/rsta.2009.0273>.
- [20] H. Heinz, C. Pramanik, O. Heinz, Y. Ding, R.K. Mishra, D. Marchon, R.J. Flatt, I. Estrela-Lopis, J. Llop, S. Moya, R.F. Ziolo, Nanoparticle decoration with surfactants: molecular interactions, assembly, and applications, *Surf. Sci. Rep.* 72 (1) (2017) 1–58, <https://doi.org/10.1016/j.surfrep.2017.02.001>.
- [21] E.M. Hotze, T. Phenrat, G.V. Lowry, Nanoparticle aggregation: challenges to understanding transport and reactivity in the environment, *J. Environ. Qual.* 39 (2010) 1909–1924, <https://doi.org/10.2134/jeq2009.0462>.
- [22] C.C. Li, C.L. Huang, Preparation of clear colloidal solutions of detonation nanodiamond in organic solvents, *Colloids Surf. A* 353 (1) (2010) 52–56, <https://doi.org/10.1016/j.colsurfa.2009.10.019>.
- [23] F. Neugart, A. Zappe, F. Jelezko, C. Tietz, J.P. Boudou, A. Krueger, J. Wrachtrup, Dynamics of diamond nanoparticles in solution and cells, *Nano Lett.* 7 (12) (2007) 3588–3591, <https://doi.org/10.1021/nl0716303>.
- [24] U. Maitra, A. Gomathi, C.N.R. Rao, Covalent and noncovalent functionalisation and solubilisation of nanodiamond, *J. Exp. Nanosci.* 3 (4) (2008) 271–278, <https://doi.org/10.1080/17458080802574155>.
- [25] X. Xu, Z. Yu, Y. Zhu, B. Wang, Effect of sodium oleate adsorption on the colloidal stability and zeta potential of detonation synthesized diamond particles in aqueous solutions, *Diam. Relat. Mater.* 14 (2005) 206–212, <https://doi.org/10.1016/j.diamond.2004>.
- [26] M. Zobel, R.B. Neder, S.A.J. Kimber, Universal solvent restructuring induced by colloidal nanoparticles, *Science* 347 (6219) (2015) 292–294, <https://doi.org/10.1126/science.1261412>.
- [27] M.V. Korobov, N.V. Avramenko, A.G. Bogachev, N.N. Rozhkova, E. Osawa, Nanophase of water in nano-diamond gel, *J. Phys. Chem. C* 111 (20) (2007) 7330–7334, <https://doi.org/10.1021/jp0683420>.
- [28] S.S. Batsanov, E.V. Lesnikov, D.A. Dan'Kin, D.M. Balakhanov, Water shells of diamond nanoparticles in colloidal solutions, *Appl. Phys. Lett.* 104 (13) (2014) 133105, <https://doi.org/10.1063/1.4870464>.
- [29] S.S. Batsanov, S.M. Gavrilkin, A.S. Batsanov, K.B. Poyarkov, I.I. Kulakova, D.W. Johnson, B.G. Mendis, Giant dielectric permittivity of detonation-produced nanodiamond is caused by water, *J. Mater. Chem.* 22 (2012) 11166–11172, <https://doi.org/10.1039/C2JM30836C>.
- [30] T.A. Dolenko, S.A. Burikov, J.M. Rosenholm, O.A. Shenderova, I.I. Vlasov, Diamond-water coupling effects in Raman and photoluminescence spectra of nanodiamond colloidal suspensions, *J. Phys. Chem. C* 116 (45) (2012) 24314–24319, <https://doi.org/10.1021/jp306803n>.
- [31] A.M. Vervald, S.A. Burikov, O.A. Shenderova, N. Nunn, D.O. Podkopaev, I.I. Vlasov, T.A. Dolenko, Relationship between fluorescent and vibronic properties of detonation nanodiamonds and strength of hydrogen bonds in suspensions, *J. Phys. Chem. C* 120 (34) (2016) 19375–19383, <https://doi.org/10.1021/acs.jpcc.6b03500>.
- [32] T. Petit, L. Puskar, T. Dolenko, S. Choudhury, E. Ritter, S. Burikov, K. Laptinskii, Q. Brustowski, U. Schade, H. Yuzawa, M. Nagasaka, N. Kusugi, M. Kurzyp, A. Venerosy, H. Girard, J.-C. Arnault, E. Osawa, N. Nunn, O. Shenderova, E.F. Aziz, Unusual water hydrogen bond network around hydrogenated nanodiamonds, *J. Phys. Chem. C* 121 (2017) 5185–5194, <https://doi.org/10.1021/acs.jpcc.7b00721>.
- [33] T. Dolenko, S. Burikov, K. Laptinskii, J.M. Rosenholm, O. Shenderova, I. Vlasov, Evidence of carbon nanoparticle-solvent molecule interactions in Raman and fluorescence spectra, *Phys. Status Solidi A* 212 (2015) 2512–2518, <https://doi.org/10.1002/pssa.201532203>.
- [34] A.M. Vervald, S.A. Burikov, I.I. Vlasov, O.A. Shenderova, T.A. Dolenko, Interactions of nanodiamonds and surfactants in aqueous suspensions, *Nanosystems: Phys. Chem. Math.* 9 (1) (2018) 49–51, <https://doi.org/10.17586/2220-8054-2018-9-1-49-51>.
- [35] O. Shenderova, A. Koscheev, N. Zaripov, I. Petrov, Y. Skryabin, P. Detkov, S. Turner, G. Van Tendeloo, Surface chemistry and properties of ozone-purified

- detonation nanodiamonds, *J. Phys. Chem. C* 115 (2011) 9827–9837, <https://doi.org/10.1021/jp1102466>.
- [36] O. Shenderova, A.M. Panich, S. Moseenkov, S.C. Hens, V. Kuznetsov, H.-M. Vieth, Hydroxylated detonation nanodiamond: FTIR, XPS, and NMR studies, *J. Phys. Chem. C* 115 (2011) 19005–19011, <https://doi.org/10.1021/jp205389m>.
- [37] J.B. Rosenholm, The structure and properties of medium-chain surfactant solutions: a case study of sodium octanoate, *Adv. Colloid Interface Sci.* 41 (1) (1992) 197–239, [https://doi.org/10.1016/0001-8686\(92\)80013-N](https://doi.org/10.1016/0001-8686(92)80013-N).
- [38] A. González-Pérez, J.M. Ruso, G. Prieto, F. Sarmiento, Temperature-sensitive critical micelle transition of sodium octanoate, *Langmuir* 20 (6) (2004) 2512–2514, <https://doi.org/10.1021/la035724d>.
- [39] K. Larsson, R.P. Rand, Detection of changes in the environment of hydrocarbon chains by Raman spectroscopy and its application to lipid-protein systems, *Biochim. Biophys. Acta* 326 (1973) 245–255, [https://doi.org/10.1016/0005-2760\(73\)90250-6](https://doi.org/10.1016/0005-2760(73)90250-6).
- [40] J.B. Rosenholm, P. Stenius, I. Danielsson, A study of micelle formation of short-chain carboxylates by laser-Raman spectroscopy, *J. Colloid Interface Sci.* 57 (3) (1976) 551–563, [https://doi.org/10.1016/0021-9797\(76\)90233-2](https://doi.org/10.1016/0021-9797(76)90233-2).
- [41] K. Larsson, Conformation-dependent features in the Raman spectra of simple lipids, *Chem. Phys. Lipids* 10 (1973) 165–176, [https://doi.org/10.1016/0009-3084\(73\)90013-3](https://doi.org/10.1016/0009-3084(73)90013-3).
- [42] B.P. Gaber, P. Yager, W.L. Peticolas, Interpretation of biomembranes structure by Raman difference spectroscopy. Nature of the endothermic transitions in phosphatidylcholines, *Biophys. J.* 21 (1978) 161–176, [https://doi.org/10.1016/S0006-3495\(78\)85516-7](https://doi.org/10.1016/S0006-3495(78)85516-7).
- [43] T.A. Dolenko, S.A. Burikov, S.A. Dolenko, A.O. Efitov, Yu.A. Mirgorod, Raman spectroscopy of micellization-induced liquid-liquid fluctuations in sodium dodecyl sulfate aqueous solutions, *J. Mol. Liq.* 204 (2015) 44–49, <https://doi.org/10.1016/j.molliq.2015.01.021>.
- [44] G.E. Walrafen, M.R. Fisher, M.S. Hokmabadi, W.-H. Yang, Temperature dependence of the low- and high-frequency Raman scattering from liquid water, *J. Chem. Phys.* 85 (12) (1986) 6970–6982, <https://doi.org/10.1063/1.451384>.
- [45] J.R. Scherer, *The Vibrational Spectroscopy of Water*, in: R.J.H. Clark, R.E. Hoster (Eds.), *Advances in Infrared and Raman Spectroscopy*, vol. 5, Hayden, London, UK, 1978, pp. 149–216.
- [46] F. Rull, J.A. de Saja, Effect of electrolyte concentration on the Raman spectra of water in aqueous solutions, *J. Raman Spectrosc.* 17 (1986) 167–172, <https://doi.org/10.1002/jrs.1250170202>.
- [47] T.A. Dolenko, I.V. Churina, V.V. Fadeev, S.M. Glushkov, Valence band of liquid water Raman scattering: some peculiarities and applications in the diagnostics of water media, *J. Raman Spectrosc.* 31 (2000) 863–870, [https://doi.org/10.1002/1097-4555\(200008/09\)31:8/9<863::AID-JRS630>3.0.CO;2-C](https://doi.org/10.1002/1097-4555(200008/09)31:8/9<863::AID-JRS630>3.0.CO;2-C).
- [48] T.A. Gogolinskaia, S.V. Patsaeva, V.V. Fadeev, The regularities of change of the 3100–3700 cm^{-1} band of water Raman scattering in salt aqueous solutions, *Dokl. Akad. Nauk SSSR* 290 (5) (1986) 1099–1103.
- [49] A.M. Amorimda Costa, C.F.G.C. Geraldes, J.J.C. Teixeira-Dias, Micellar aggregation of CTAB in water and chloroform solutions – a study by laser Raman spectroscopy, *J. Colloid Interface Sci.* 86 (1) (1982) 254–259, [https://doi.org/10.1016/0021-9797\(82\)90063-7](https://doi.org/10.1016/0021-9797(82)90063-7).
- [50] J. Sebek, L. Pele, E.O. Potmaand, R.B. Gerber, Raman spectra of long chain hydrocarbons: anharmonic calculations, experiment and implications for imaging of biomembranes, *Phys. Chem. Chem. Phys.* 13 (2011) 12724–12733, <https://doi.org/10.1039/c1cp20618d>.
- [51] R. Prasher, P. Bhattacharya, P.E. Phelan, Brownian-motion-based convective-conductive model for the effective thermal conductivity of nanofluids, *J. Heat Transfer* 128 (2006) 588, <https://doi.org/10.1115/1.2188509>.
- [52] S. Krishnamurthy, P. Bhattacharya, P.E. Phelan, R.S. Prasher, Enhanced mass transport in nanofluids, *Nano Lett.* 6 (2006) 419–423, <https://doi.org/10.1021/nl0522532>.
- [53] M. Picquart, G. Lacrampe, Raman spectra of aqueous sodium octanoate solutions: solute and solvent study, *J. Phys. Chem.* 96 (23) (1992) 9114–9120, <https://doi.org/10.1021/j100202a009>.
- [54] H. Okabayashi, M. Okuyama, T. Kitagawa, The Raman spectra of surfactants and the concentration dependence of their molecular conformations in aqueous solutions, *Bull. Chem. Soc. Jpn.* 48 (1975) 2264–2269, <https://doi.org/10.1246/bcsj.48.2264>.
- [55] J. Umemura, D.G. Cameron, H.H. Mantsch, FT-IR study of micelle formation in aqueous sodium N-hexanoate solutions, *J. Phys. Chem.* 84 (1980) 2272–2277, <https://doi.org/10.1021/j100455a012>.